University of Exeter coursework header sheet

ECM3101 Individual Project (Beng) (A, TRM1+2 2015/6)

010202

1019472

630017693

Coursework: Final Report

Submission Deadline: Thu 28th Apr 2016 12:00

Personal tutor: Dr Guangtao Fu

Marker name: G Tab

Word count: 7573

By submitting coursework you declare that you understand and consent to the University policies regarding plagiarism and mitigation (these can be seen online at www.exeter.ac.uk/plagiarism, and www.exeter.ac.uk/mitigation respectively), and that you have read your school's rules for submission of written coursework, for example rules on maximum and minimum number of words. Indicative/first marks are provisional only.

Final Report

Investigation of a Compact 3D Heat Exchanger with the aid of Experimental and Computational Techniques

Andrew James Farley

2016

3rd Year Individual Project

I certify that all material in this thesis that is not my own work has been identified and that no material has been included for which a degree has previously been conferred on me.

Signed..... 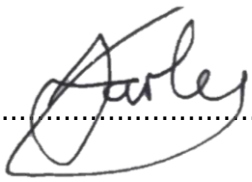 .....

College of Engineering, Mathematics, and Physical Sciences
University of Exeter

Final Report

ECM3101

Title: Investigation of a Compact 3D Heat Exchanger with the aid of Experimental and Computational Techniques

Word count: 7573

Number of pages: 29

Date of submission: Wednesday, 27 April 2016

Student Name: Andrew James Farley

Programme: BEng Mechanical Engineering

Student number: 630017693

Candidate number: 010202

Supervisor: Dr Gavin Tabor

Abstract

Heat exchangers are devices that are used to transfer heat between one or more fluids, and can be found in a wide variety of real world systems. Their purpose is to help improve the efficiency of such systems. This project aims to analyse a compact heat exchanger that has been provided by the engineering technology firm HiETA Technologies Ltd, using appropriate experimental and computational analysis techniques.

In particular, the project will focus on the pressure drop across the heat exchanger in question, whilst the computational models will use porous media modelling theory as an alternative modelling method. Porous media modelling will hopefully provide an accurate replica of the internal structure of the heat exchanger whilst significantly reducing computation time due to the decreased complexity of the model.

The project will also attempt to identify the optimal operating conditions for this heat exchanger, taking into consideration factors such as inlet flow velocity, mean temperature efficiency and pressure drop.

The accuracy and precision of any experimental or computational results gained will be examined in order to ensure the reliability of the project.

Any potential future research will be discussed at the end of the project, as well as all sustainability, environmental and socio-economic issues related to the subject matter.

Keywords: heat, exchange, porosity, pressure, CFD

Table of contents

1. Introduction and background

1.1. Heat Exchanger Background

In its most simple terms, a heat exchanger is a unit designed to transfer heat from one medium to another via conduction. There are several different types of heat exchanger which all come in varying shapes and sizes, and uses of heat exchangers can be found in many different aspects of life – from the natural world (i.e. the human nasal passage) to industrial uses (refrigeration, waste water treatment, etc.). In the following sections are descriptions of some of the main types of heat exchanger and how they each differ from one another.

1.1.1. Shell and Tube

A shell and tube heat exchanger is made of a cylindrical shell, inside which are mounted a number of tubes. Both the cylindrical shell and internal tubes contain fluids which then flow past one another – in either a concurrent flow or countercurrent flow – and exchange heat. Shell and tube heat exchangers are one of the most widely used types of heat exchanger because there is an extremely wide range of pressures and temperatures for which they are suitable.

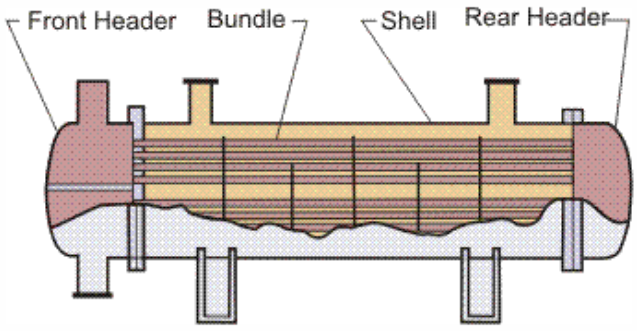

Figure 1 - Shell and tube heat exchanger diagram **[1]**

1.1.2. Plate

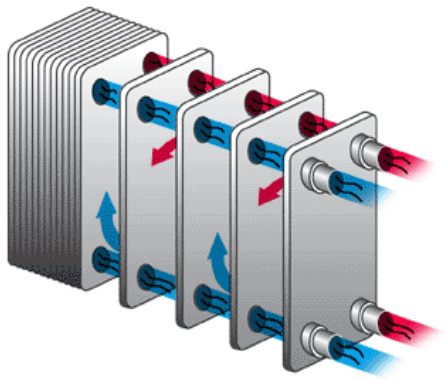

Figure 2 – Plate heat exchanger diagram **[2]**

Plate heat exchangers are cheap and flexible; at the same time they are easy to maintain. They are made up of a number of gasketed plates that are fixed between top and bottom carrying bars, and flow enters the heat exchanger through frame connections. The plates are heated and act as a medium for heat transfer between two fluids, which is particularly efficient due to the large surface area of the plate to which the fluids are exposed.

1.1.3. Spiral

A spiral heat exchanger consists of two long metal plates which are rolled around a centre core, forming two concentric spiral passages. Each spiral passage contains one fluid, and the plate edges are welded shut so that there is no bypassing or mixing of flows. Spiral heat exchangers have a high thermal efficiency and can also be operated in countercurrent or concurrent flow.

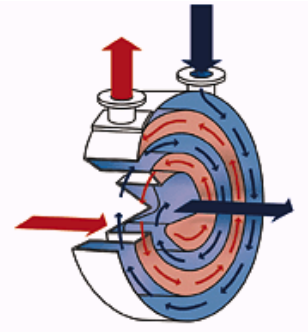

Figure 3 - Spiral heat exchanger diagram **[3]**

1.1.4. Adiabatic Wheel

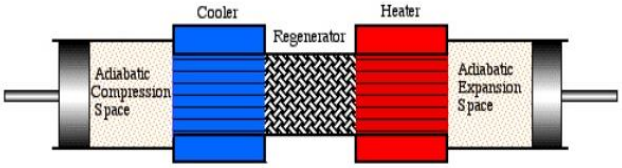

Figure 4 - Adiabatic wheel heat exchanger diagram **[4]**

In an adiabatic wheel heat exchanger, heat is transferred from one side of the exchanger unit to the other via an intermediate fluid which is used for the storage of heat. A large wheel is then rotated through the hot and cold fluids in order to either transfer or extract heat.

1.2. HiETA Technologies Ltd.

HiETA Technologies Ltd. is a 'product design, development and production company exploiting the new technology of Additive Manufacturing (AM)' [5]. The company is based in Bristol, and works across fields including design services and design engineering as well as working on a number of different case studies and collaboration projects. Specifically, these case studies focus on the automotive, defence, and heat exchangers and engines sectors.

Presently, the heat exchangers and engines division is working hard to challenge and shift current thinking regarding the performance of compact heat exchangers, and is creating highly efficient, light and complex products that are able to increase performance at a reduced weight. At this time, some core application areas of HiETA include waste heat recapture & power generation, auxillary power units (APUs) and aerospace & electronic cooling.

One of HiETA's most recent projects involved the design and manufacture of a compact shell and tube heat exchanger, and this heat exchanger formed the basis for this project. Images of the manufactured heat exchanger can be seen below in Figure 5.

Figure 5 - Images of the HiETA heat exchanger

This model was manufactured using additive manufacturing techniques and has approximate dimensions of 170x70x45mm. There are roughly 300 internal tubes, each with an internal diameter of 1mm and a wall thickness of 0.5mm.

1.3. Project Scope

The main aim of this project was to analyse the properties of the heat exchanger which had been provided by HiETA Technologies Ltd. The purpose was to provide performance data – specifically pressure drop at varying flow rates – as well as optimal operating conditions for the heat exchanger design, whilst ensuring that the data provided was as reliable as possible.

Upon further consideration, it was also decided that the internal structure of the heat exchanger would be modelled as a porous region. The reasoning behind this was that the model is a shell and tube heat exchanger, but there are so many internal tubes that are so tightly packed together that they behave in a similar fashion to that of a porous zone. In addition, due to the intricacy of the internal structure, porous media modelling would decrease the complexity of any future simulations and this would provide an interesting set of results for comparison to any experimental findings.

1.4. Project Structure

This project is split into two main sections, one in which experiments are designed and carried out, and one section in which the heat exchanger is modelled and analysed using computational fluid dynamics.

In order to be able to conduct any experimentation or modelling, prior research is required. This includes a literature review as well as a methodology and theory section. The purpose of the literature review is to identify any work that has previously been done in and around the field of porous media modelling of heat exchangers and use this information to shape the project as a whole.

The methodology and theory section is dedicated to researching the fundamentals of the project. This is in order to ensure a clear understanding of the topic, as well as clarification of any analysis techniques that were to be used after experimental and computational results had been taken.

After the methodology and theory section, the experimental and computational methods within the project are outlined in much greater detail in the experimental work and analytical investigation section. This includes details of all processes and instructions used to conduct any experimental or modelling work.

The experimental and computational results are then presented in the experimental and analytical results section, before the project is summarised within the discussion and conclusions section.

Finally, a project management section includes details of any sustainability or health and safety factors as well as a Gantt chart to illustrate the sequencing of project tasks.

2. Literature review

2.1. Heat Exchanger Pressure Drop

Pressure drop across a heat exchanger is an extremely important property associated with heat exchange, and needs to be taken into consideration when designing modern day heat exchangers. Shah and Sekulic [6] discuss the importance of heat exchanger pressure drop, in particular how a large pressure drop will affect the temperature potential for heat transfer. As demonstrated by Equation 1, pressure drop is proportional to the fluid pumping power of the pump in the system. A heat exchanger with an especially large pressure drop will require a high fluid pumping power, and this will further reduce the efficiency of the exchange.

$$\mathcal{P} = \frac{\dot{V}\Delta p}{\eta_p}$$

Equation 1 – $\mathcal{P}$ = fluid pumping power; $\dot{V}$ = volumetric flow rate; p = pressure; η_p = pump efficiency

As a result of this information, the project aimed to identify optimal operating conditions for the heat exchanger – with particular consideration of pressure drop at different flow rates.

In 2010, Mohammed M. Farid [7] spoke about the use of baffles in shell and tube heat exchangers to ensure the flow of shell-side fluid over every single tube. The design of these baffles also means that the turbulence of the shell-side flow is increased, which subsequently increases the rate of heat transfer – but poor baffle design can cause flow stagnation which results in lowered heat transfer coefficients within the flow. The recent technological advancements made by HiETA Technologies Ltd. [5] have led to the manufacture of the heat exchanger used in this project, which features a baffle free design. Due to this lack of baffles, the shell-side flow of the heat exchanger was not undular and as such no analysis of the impact of baffling was to be undertaken.

2.2. Porous Media Modelling

Sobieski [8] conducted research into the differences between the porous media model (PMM) and the Eulerian Multiphase model (EMM) in fluid-solid systems. The important characteristic to note is whether or not the particles of solid body are stationary. In the porous media model, the case is evaluated with typical fluid flow through a porous bed, whereas EMM relies on

analysis of fluid flow through a non-stationary porous bed.

Due to the nature of heat exchangers in general the solid body will not have any movement, and as such any computational fluid dynamics simulations in this project will require use of the porous media model rather than the use of the Eulerian Multiphase model.

The ANSYS Fluent User Guide [9] provides important information regarding the setup of the porous media model. Section 7.2.3 details all processes required for correct use of the PMM, including treatment of the energy equation, treatment of turbulence and user inputs for porous media. In particular, the user guide outlines the definition of viscous and inertial resistance coefficients. Viscous resistance takes into account any frictional losses characterized by the fluid viscosity and the structure of the porous matrix, whilst inertial resistance is related to the losses associated with expansion, constriction and bends in the pore channels [10]. These viscous and inertial resistance coefficients can be arranged to form a modified Darcy equation, shown in Equation 2.

$$-\frac{dp}{dy} = \alpha\eta V + \beta\rho V^2$$

Equation 2 – α = viscous resistance coefficient; η = fluid viscosity; V = superficial velocity of fluid flow; β = coefficient of inertia; ρ = density

The viscous and inertial resistance effects of the porous media must be taken into consideration when setting up the internal fluid conditions of the HiETA heat exchanger because there will be a relevant Darcy matrix to define the direction of resistance. Due to the fact that the porous region in the HiETA heat exchanger consists of horizontal pipes, the porous zone will be anisotropic and as such an appropriate Darcy's law matrix needs to be set up to determine the directions and magnitudes of resistance to flow within the porous region. The methodology behind this is discussed in the Compass porous media manual [11].

3. Methodology and theory

As previously mentioned, the project was split into two main sections: experimental and modelling. The experimental section was also then divided further into two separate experiments - one to determine the inlet and outlet temperatures of the heat exchanger at different water flow rates, the other to determine the pressure drop across both the hot and cold water circuits. The aim of the first experiment was to provide boundary conditions for the

computational models that were to be simulated, whilst the second experiment was to validate any results gained through modelling.

3.1. Experimental Theory

The experiments were designed in order to investigate the temperature change and pressure drop across the heat exchanger in both concurrent and countercurrent flow at a constant cold water flow rate with varying hot water flow rates. The results of these were then manipulated in a number of different ways in order to provide important information with regards to the performance characteristics of the heat exchanger.

Firstly, the logarithmic mean temperature difference (LMTD) was determined. LMTD is a measure of the temperature driving force for heat transfer in systems of flow and is most commonly used for analysis of heat exchangers [12]. The formula for LMTD can be seen below in Equation 3.

$$LMTD = \frac{\Delta T_A - \Delta T_B}{\ln\left({}^{\Delta T_A}/_{\Delta T_B}\right)}$$

Equation 3 - T_A=temperature difference between the two inlet streams; T_B=temperature difference between the two outlet streams

A higher LMTD value equates to a greater amount of heat transferred.

After this, the power emitted by the hot water, Q_e, and the power absorbed by the cold water, Q_a, were calculated. The formulae for these can be found in Equation 4 below.

$$Q_e = m_h c_{p_{hot}}(T_x - T_y)$$

$$Q_a = m_c c_{p_{cold}}(T_y - T_x)$$

Equation 4 - m_h= hot water mass flow rate; m_c= cold water mass flow rate; c_p= specific heat of water; T_x= temperature difference between hot water inlet and outlet; T_y= temperature difference between cold water inlet and outlet

The specific heat of water at 50°C is 4.182kJ/kg K, whilst at 10°C the specific heat of water is 4.186kJ/kg K.

Another tool for analysis was the temperature efficiencies of the hot and cold water and the mean temperature efficiency. The equations for all three of these values can be seen in Equation 5 below.

$$\eta_h = \frac{T_x}{T_A} \times 100\%$$

$$\eta_c = \frac{T_y}{T_B} \times 100\%$$

$$\eta_m = \frac{\eta_h + \eta_c}{2}$$

Equation 5 – $\eta_h = temperature\ efficiency\ of\ hot\ water$; $\eta_c = temperature\ efficiency\ of\ cold\ water$; $\eta_m = mean\ temperature\ efficiency$

The penultimate piece of information to be gained was the overall heat transfer coefficient, U, of the heat exchanger for the given flow rates, and this was determined using Equation 6 below.

$$U = \frac{Q_e}{A \times LMTD}$$

Equation 6 – A = heat transmission area

Typical values for the overall heat transfer coefficient of a heat exchanger with water as the fluid range from approximately 900-2500 W/m²K **[13]**, so it was anticipated that the experimental values would fall within this region. The heat transmission area of the heat exchanger was 0.002573m².

Finally, for the pressure drop experiment results would be recorded from a manometer and would therefore give values in millimetres. In order to convert these values to a pressure value, Equation 7 needed to be used.

$$P = \rho g h$$

Equation 7 - P = pressure; ρ = density; g = acceleration due to gravity; h = height of water

The density of water at 50°C is 988 kg/m³, whilst it is 999.7 kg/m³ at 10°C **[14]**. The value of g was taken as 9.81 m²/s.

3.2. Modelling Theory

3.2.1. Heat Exchanger Geometry

The computational model was to be run within ANSYS Fluent, using a CAD model of the heat exchanger which had been provided by HiETA. However, the geometry of this model was far too complex to create an appropriate mesh as it contained every feature of the heat exchanger, including the internal tubes and detailed inlet and outlet manifolds. Instead, a simplified replica CAD model was created using SolidWorks, with the dimensions provided in the original model acting as a guide for the general geometry of the new model. This second model was created as a solid part which followed the same external geometry but, due to the fact that it did not contain any of the internal tubes, it was far simpler. A comparison of the cross sections of each model can be seen below, in Figure 6.

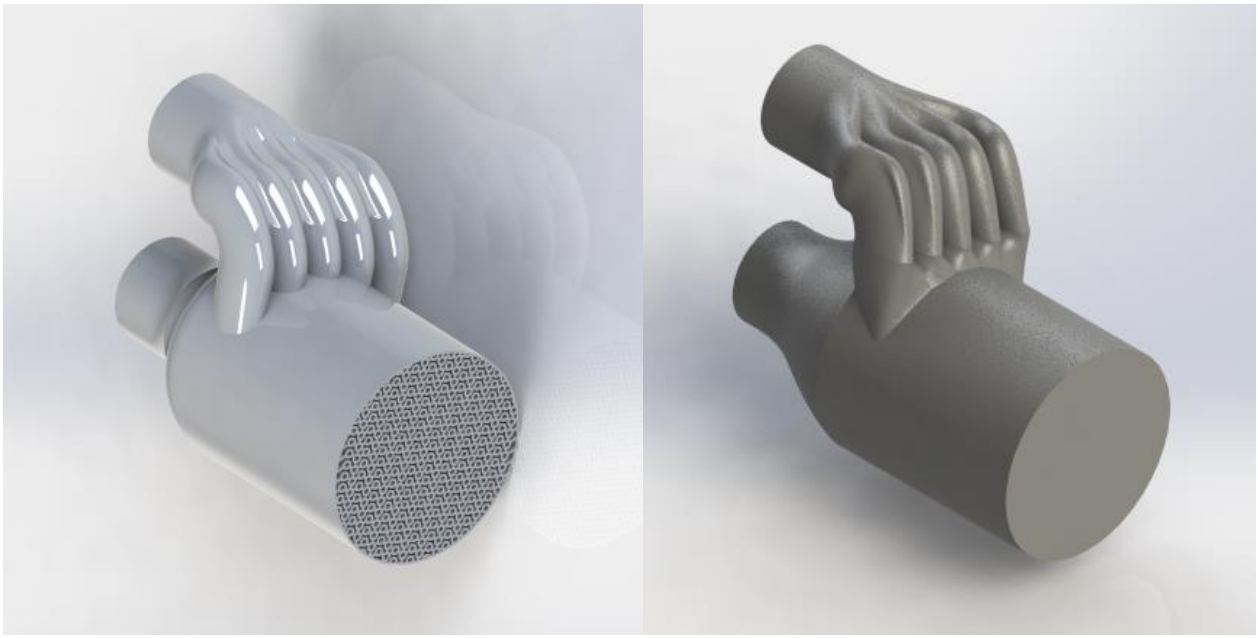

Figure 6- Cross-section comparison; original model (left) vs simplified model (right)

Despite the simplifications of the second model, there were still some intricate geometries around the inlet and outlet manifold sections which caused problems whilst attempting to create a mesh within ANSYS. As a result of this, a third model was created – in which the inlet and outlet manifold sections were simplified in order to remove any complex geometry. A comparison of the three models can be seen in Figure 7 below.

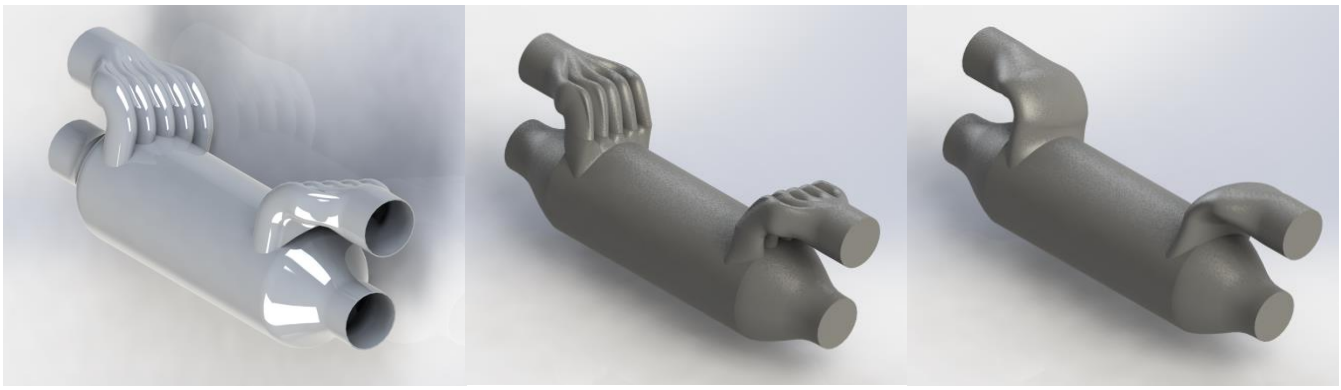

Figure 7 - Model comparison; original model (left) vs second model (centre) vs final model (right)

3.2.2. Heat Exchanger Porosity

Using ANSYS Fluent, the heat exchanger was to be modelled as a porous zone rather than as a shell and tube heat exchanger. The reason for this was that the heat exchanger is, by definition, a shell heat exchanger containing lots of tubes; however, there are so many tubes that are so small that this section can effectively be treated as a porous zone.

Before the model could be analysed, the porosity of each section needed to be estimated. Porosity is defined as a measure of the empty spaces within a material [15], and can be calculated using Equation 8. It is a ratio of volumes and is therefore dimensionless. This equation will give a value between 0 and 1, where a porosity of 1 means the region is all fluid with no solid. A porosity of 0 means the region is all solid with no fluid.

$$\Sigma = \frac{V_V}{V_T}$$

Equation 8 – Σ=porosity, V_V = voids volume, V_T = total volume

The heat exchanger itself was modelled as two separate sections – the central section, which was for the hot water circuit, and the manifold section, which was for the cold water circuit – and as a result of this two different values of porosity needed to be calculated.

For the cold water circuit, the voids volume was taken as the internal volume of the tubes running through the heat exchanger, which was found to be 1.5315×10^{-5}m³. The total volume of the porous zone was taken as the total volume filled by the tubes running through the heat exchanger, which included the tube wall thickness. The value of this was 6.126×10^{-5}m³, meaning that the total porosity for this section was 0.25.

The total volume of the hot water circuit was taken as 1.3757×10^{-4}m³, whilst the voids volume for this section was the total volume minus the volume filled by the tubes running through the section. The volume of the tubes being 6.126×10^{-5}m³ meant that the voids volume was 7.631×10^{-5}m³, and thus the porosity of the central section was 0.555.

3.2.3. Reynold's Number

Having calculated the porosity of the heat exchanger, the next step was to calculate Reynold's number for the flow so that the most appropriate turbulence model could be chosen on ANSYS Fluent. The equation for Reynold's number in a pipe flow can be found in Equation 9 below.

$$Re = \frac{U \times d_h}{\nu}$$

Equation 9 - Re = Reynold's number; U = flow velocity; d_h = hydraulic diameter; ν = kinematic viscosity

The value for Reynold's number was calculated at both the hot and cold water circuit inlets, which each had a hydraulic diameter of 0.01m. However, the volumetric flow rate and kinematic viscosity at each inlet varied – at the hot water inlet the flow velocity ranged between 1.432m/s and 7.639m/s with a kinematic viscosity of 5.54×10^{-7}m²/s, whilst at the cold water inlet the flow velocity also varied between 1.432m/s and 7.639m/s but with a kinematic viscosity of 1.31×10^{-6}m²/s. These conditions resulted in Reynold's numbers ranging from approximately 25500 for the lowest inlet flow velocity to approximately 138000 for the highest inlet flow velocity.

Reynold's number in all cases here is greater than 4000, meaning that the flow is turbulent. The standard k-ε turbulence model was selected as it is the most commonly used model, valid only for fully turbulent flows, and it will provide accurate results with a relatively low computation time when compared to the other, more complex turbulence models.

3.2.4. Mesh Refinement Study

The final stage in preparation for the modelling process was to conduct a mesh refinement study. Increasing the mesh density will increase the accuracy of results but it will also increase the simulation time, so the purpose of this mesh refinement study was to find a mesh density

that would provide the most accurate simulations whilst retaining a reasonable balance between precision and computation time.

Due to the fact that the final CAD model was made using two main sections and the majority of simulations were to be run as two separate sections, two separate mesh refinement studies were undertaken – one for the hot water circuit and one for the cold water circuit of the heat exchanger. The results of this study can be seen below, in Table 1 and Figure 8.

Element Sizing	No. of Nodes	No. of Elements	ΔP_{cold}	ΔP_{hot}
mm	-	-	*kPa*	
5.00	4422	3384	297.34	19.04
2.50	24563	22152	285.65	19.54
2.00	36658	67928	271.49	19.61
1.50	82413	260829	261.96	19.77
1.10	134762	512106	262.53	19.94
0.90	197896	1033608	262.23	20.03
0.75	283147	1486183	262.35	20.05

Table 1 - Table of Results; Mesh Refinement Study

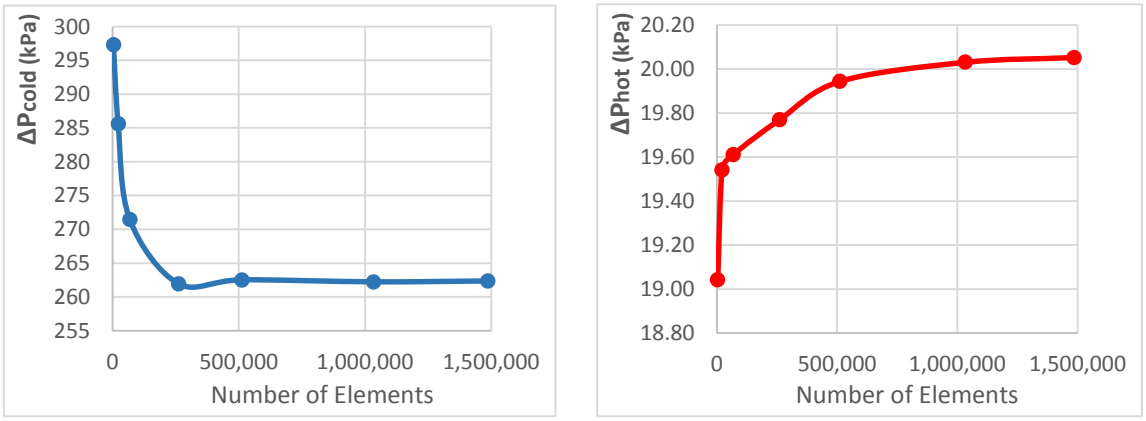

Figure 8 - Graphs showing mesh refinement studies for cold water circuit (left) and hot water circuit (right)

From the graphs above, it is clear that both the hot and cold water circuits had convergent results in this mesh refinement study. The results for the cold water circuit converged at roughly 100000 nodes, whilst the results for the hot water circuit converged at just over 200000 nodes. Consequently, element sizes of 1.50mm and 0.90mm were used for the cold water circuit and hot water circuit respectively whilst carrying out the final simulations.

4. Experimental work and analytical investigation

4.1. Temperature Change Experiment

4.1.1. Preliminary Work

The first experiment was performed using an Armfield HT30X heat exchanger service unit. However, the tubes on this machine were too thin to fit directly onto the heat exchanger provided by HiETA so some preliminary work had to be undertaken before the experiment could take place. In order to ensure that the heat exchanger could be connected into the HT30X service unit, four adaptors were designed and then machined out of plastic using a lathe. A photograph of one of the manufactured parts can be seen in Figure 9 to the left.

Figure 9 - Photograph of manufactured adaptor

These adaptors were designed so that one end would slot into a larger diameter pipe that fit directly onto the heat exchangers, whilst the other end would slot into the pipes of the HT30X service unit. Drilled through the whole part was a 7mm hole to allow for the flow of water, whilst 5mm holes were drilled into the centre of the adaptor in order to allow for tapping to be added so that pressure drop could also be recorded. A photograph of the tapping can be seen in Figure 10 to the right.

Figure 10 - Photograph of adaptor with tapping

4.1.2. Experimental Method

The heat exchanger was set up in concurrent flow on the HT30X heat exchanger service unit. The temperature was set to 25°C using the set button on the control console, before the system was primed.

The temperature controller was then increased to 50°C, and the hot water circulating pump was switched on. Next, the hot and cold water control valves were adjusted in order to give flow rates of 3 litres per minute and 0.45 litres per minute respectively. Once the temperatures had stabilised, T1, T2, T3, T4, F_{cold} and F_{hot} were recorded. These steps were then repeated at hot

water flow rate intervals of 0.15 litres per minute – up to a flow rate of roughly 2.4 litres per minute. The cold water flow rate was kept constant at 3 litres per minute throughout the entire experiment.

After all 14 results had been measured, the hot water circulating pump was switched off and the system was left to cool down for several minutes. The connections were then changed so that the heat exchanger was set up in countercurrent flow, and the same experimental procedure was repeated.

4.2. Modelling Process

The computational modelling was performed using ANSYS Fluent on which studies into the pressure drop across each section were undertaken. Two sets of simulations were performed, half on just the central section of the heat exchanger and half on just the manifold section. Each final simplified geometry was imported from SolidWorks, and named selections were created for the inlets, outlets and walls of the models. A mesh was then created onto this geometry, using the mesh densities identified in the mesh refinement study – with element sizes of 1.50mm and 0.90mm for the cold water circuit and hot water circuit respectively. Images of these meshes on each simplified SolidWorks model can be found below in Figure 11.

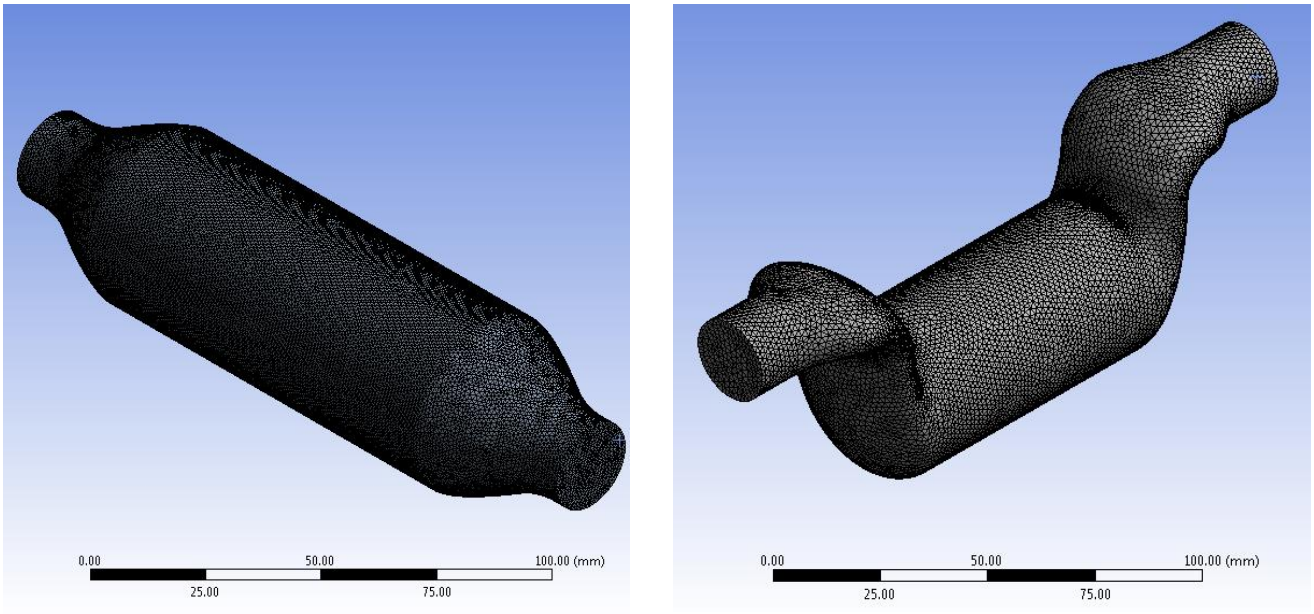

Figure 11 - Final meshes for hot water circuit (left) and cold water circuit (right)

To set up the simulation, the viscous model was set to standard k-ε. There was no need to turn on the energy equation because each section was to be analysed for pressure drop individually, and thus any changes in temperature would not have had a significant impact. Both the cold and hot water circuits were then adjusted so that the internal fluid was water, and each section was set as a porous zone with respective porosities of 0.25 and 0.555 – as discussed earlier in section 3.2.2. The boundary conditions were different for each case, and were determined using the flow velocities and mass flow rates from the temperature change experiment. Table 2 below shows the conditions for each setup of simulations. The same flow velocities and mass flow rates were used for both the hot and cold water circuits so that the pressure drop across each could be compared to one another.

Once the boundary conditions had been input, all residuals were set to an absolute criteria of 0.00001, and the simulation was initialized. Each solution was run for 1000 iterations, or until the solution had converged fully.

Inlet Flow Velocity	Outlet Mass Flow Rate
m/s	*kg/s*
1.432	0.445
1.910	0.603
2.387	0.751
2.865	0.889
3.342	1.037
3.820	1.186
4.297	1.354
4.775	1.492
5.252	1.630
5.730	1.778
6.207	1.927
6.685	2.075
7.162	2.243
7.639	2.361

Table 2 - Simulation boundary conditions

4.3. Pressure Drop Experiment

The heat exchanger was set up in concurrent flow on the HT30X heat exchanger service unit. The hot and cold water circuit pressure tappings were then attached to an energy losses in bends and fittings manometer board, like the one shown in Figure 12. These connections were arranged so that the manometer board would provide readings for pressure drop across both the hot water circuit and the cold water circuit of the heat exchanger.

Figure 12 – Image of energy losses in bends and fittings circuit

The temperature was set to 25°C using the set button on the control system, before the system was primed. The temperature controller was then increased to 50°C and the hot water circulating pump was switched on. After this, the hot and cold water control valves were adjusted in order to give flow rates of 3 litres per minute and 0.45 litres per minute respectively. When the manometer values had settled, the height of the water within the manometer was measured - providing readings for hot water inlet head and hot water outlet head in millimetres. The hot water flow rate was then increased by 0.15 litres per minute and the measurement procedure was repeated until as many results as possible had been recorded.

After this, the hot water flow rate was reduced to 0.45 litres per minute and the cold water inlet and outlet head was measured. The cold water flow rate was then decreased at intervals of 0.15 litres per minute and readings for inlet and outlet head were measured until as many measurements as possible had been taken.

It is important to note that it was not possible to record results for each flow rate used in the CFD. The reason for this was that, because the energy losses in bends and fittings manometer board was not designed for this experiment, certain hot or cold water flow rates did not provide sufficient pressure to give a reading on the manometer board. As a result of this, only measurements between 1.05 – 2.70 litres per minute could be taken for the cold water circuit, whilst for the hot water circuit readings were taken between 0.45 – 1.8 litres per minute.

5. Presentation of experimental and analytical results

5.1. Temperature Change Experimental Results

The results of the temperature change experiment can be found in Figures 13 and 14 below, as well as in Appendix A, Tables 4 and 5.

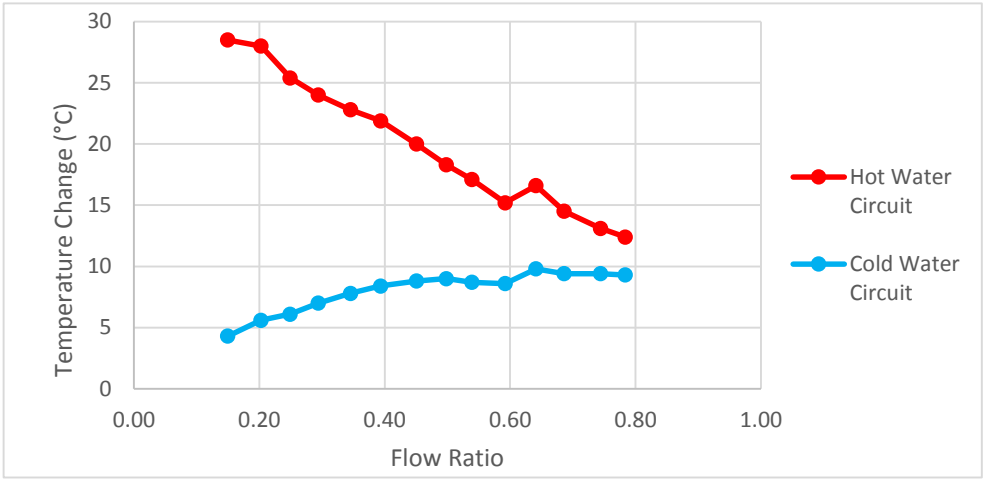

Figure 13 - Graph to show temperature change across the heat exchanger unit for varying hot water flow rates in concurrent flow

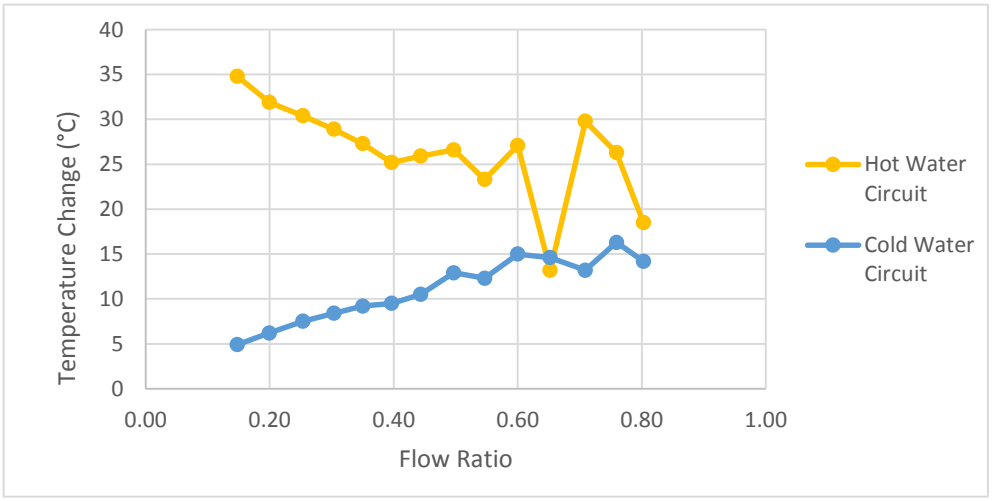

Figure 14 - Graph to show temperature change across the heat exchanger unit for varying hot water flow rates in countercurrent flow

From the graphs above, it is clear that the temperature change in both the hot and cold water circuits was more significant when the heat exchanger was arranged in countercurrent flow. At the lowest flow ratio in concurrent flow, the temperature change was 28.5°C and 4.3°C across the hot and cold water circuits respectively – whilst in countercurrent flow these temperature

changes increased to 34.8°C and 4.9°C.

In addition, it is evident that as the flow ratio is increased the temperature change across the hot water circuit decreases whilst the temperature change across the cold water circuit increases. This is because the cold water flow rate stays the same throughout the whole experiment whilst the hot water flow rate is gradually increased. As the hot water flow rate is increased, the hot water spends a shorter amount of time in contact with the cold water circuit so has less time to cool; thus the hot water outlet temperature remains higher and the temperature change across the hot water circuit is decreased. The temperature change across the cold water circuit increases because at higher hot water flow rates there is a greater volume of hot water coming into contact with the cold water circuit – meaning the amount of energy transferred is greater and thus the cold water circuit temperature change increases. This is supported by further analysis of the results to calculate power absorbed by the cold water, Q_a, which increases as the flow ratio increases – as shown in Tables 4 and 5 in Appendix A.

Also shown in Tables 4 and 5 in Appendix A are the calculated temperature efficiencies of the hot water and cold water circuits, η_h and η_c, as well as the mean temperature efficiency, η_m, which confirm that the heat exchanger was more effective in a countercurrent arrangement than when it was set up in concurrent flow. The highest mean temperature efficiency of the heat exchanger whilst in concurrent flow was 62%, whilst in countercurrent flow it had several values greater than 90%. In two countercurrent cases, the mean temperature efficiency was over 100%, but this is discussed later in the discussion and conclusions section.

Values for the overall heat transfer coefficient, U, of the heat exchanger were also calculated and can be seen in Tables 4 and 5 in Appendix A for both concurrent and countercurrent flows. On the whole the overall heat transfer coefficient increased with the flow ratio, although it was higher when the heat exchanger was setup in countercurrent flow – ranging from roughly 3000-9000 W/m²K whilst in concurrent flow values ranged between 1200-3000W/m²K.

5.2. Pressure Drop Simulations

The results provided by all simulations can be seen in Figure 15 as well as Table 6 in Appendix B.

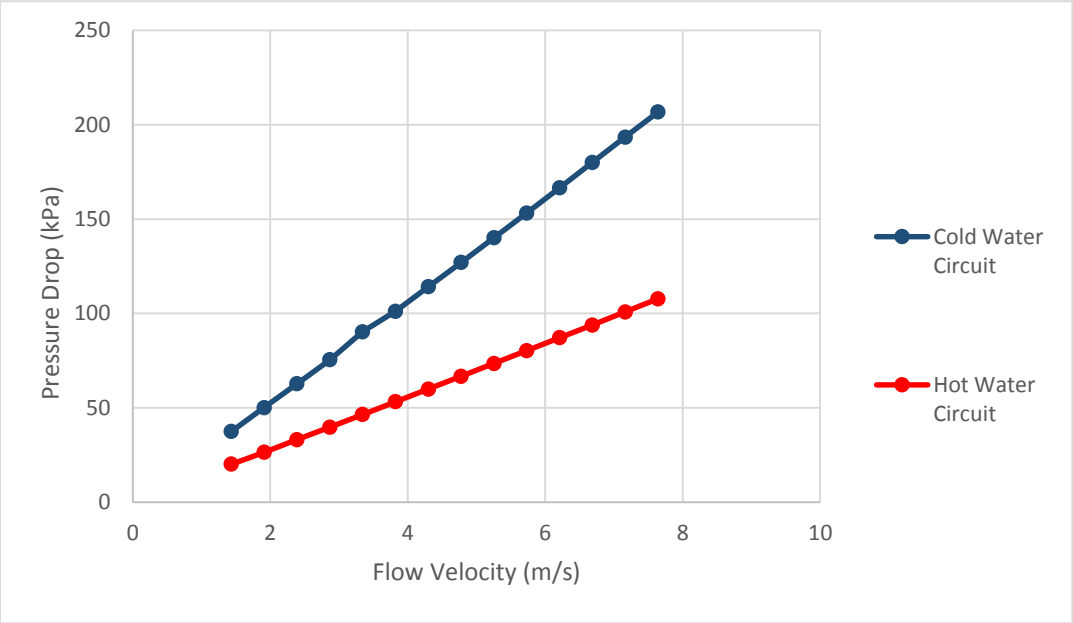

Figure 15 – Graph to show simulated pressure drop against flow velocity for both the hot water and cold water circuit of the heat exchanger model

From the graph above, it is clear that the pressure drop across the cold water circuit was greater than the pressure drop across the hot water circuit for all flow velocities that were simulated. In fact, both plots are straight lines which suggests that – for these simulations – pressure drop was proportional to flow velocity. However, the gradient of the cold water circuit line was steeper than the gradient of the hot water circuit line, which shows that pressure drop increased with flow velocity at a higher rate for the cold water circuit.

Images showing filled contours of total pressure for each circuit can be seen in Figure 16.

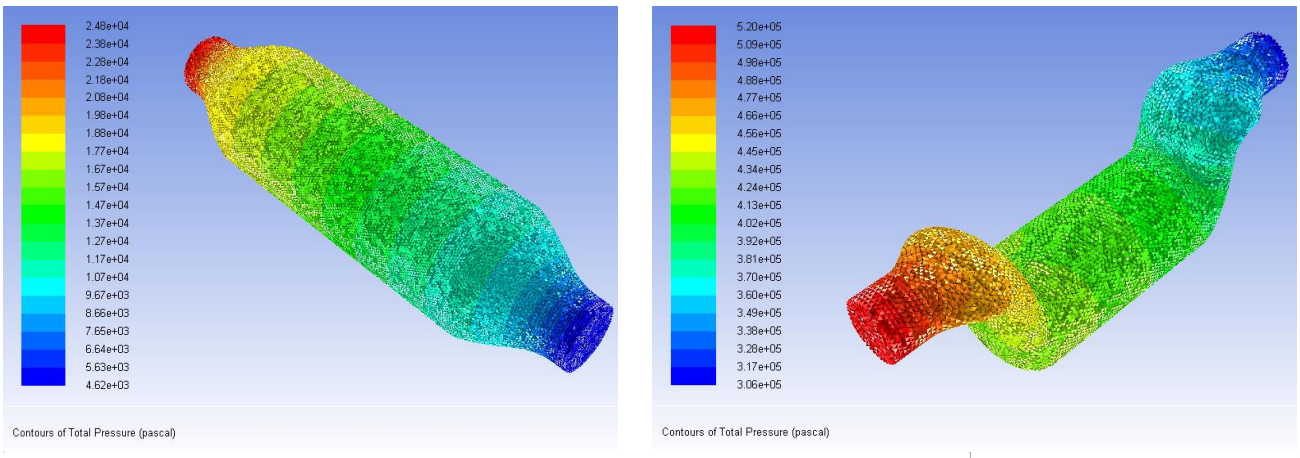

Figure 16 - Filled contours of total pressure for hot water circuit (left) and cold water circuit (right)

5.3. Pressure Drop Results Comparison

The graphs in Figures 17 and 18 below show comparisons of the experimental and simulated results for pressure drop across the hot and cold water circuits of the heat exchanger. Table 3 below shows the simulation pressure drop results and experimental pressure drop results side by side, and Table 7 in Appendix C shows the experimental data taken from the pressure drop practical.

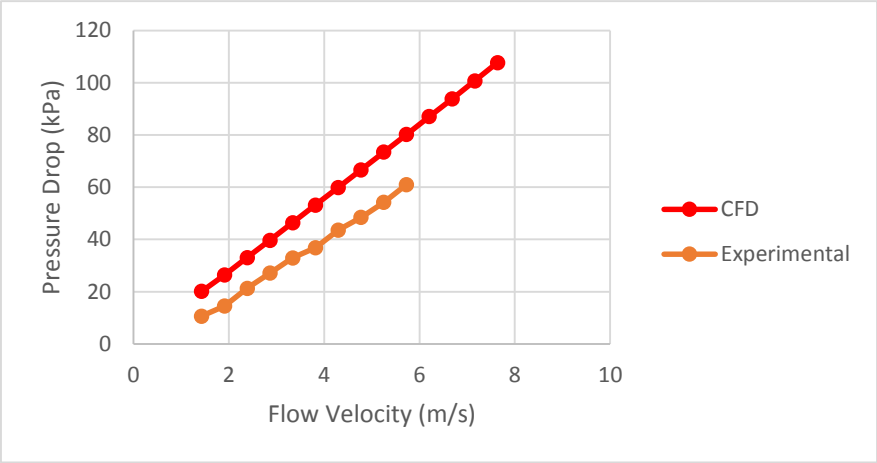

Figure 17 - Graph to show simulated and experimental pressure drop against flow velocity for the hot water circuit

From the graph in Figure 17, it is clear that the simulated values of pressure drop across the hot water circuit are greater than the values gained through experimental work. However, the difference between the two values increases gradually with flow velocity – at a flow velocity of 1.432m/s the difference is roughly 10kPa, whereas by the time the flow velocity has been increased to 5.730m/s the difference has increased to approximately 19kPa.

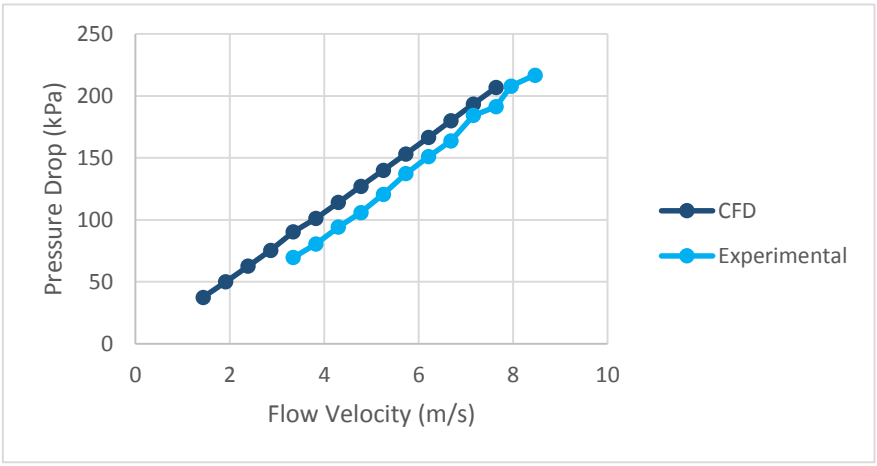

Figure 18 - Graph to show simulated and experimental pressure drop against flow velocity for the cold water circuit

In Figure 18 it can be seen that the pressure drop values from CFD are also higher than the results gained experimentally for the cold water circuit. However, the cold water circuit experimental results appear to follow the simulated results more accurately than in the case of the hot water circuit in Figure 17. By looking at Table 3 it becomes clear that the difference between the two curves for the cold water circuit is actually slightly greater than that of the hot water circuit – ranging between 15-20kPa. In spite of this, the difference seems smaller because the numbers being dealt with are – on the whole – larger.

Volumetric Flow Rate	Flow Velocity	*CFD*		*Experimental*	
		ΔP_{cold}	ΔP_{hot}	ΔP_{cold}	ΔP_{hot}
m^3/s	m/s	*kPa*		*kPa*	
0.00045	1.432	37.413	20.138	-	10.662
0.00060	1.910	50.036	26.392	-	14.538
0.00075	2.387	62.700	33.084	-	21.323
0.00090	2.865	75.460	39.740	-	27.138
0.00105	3.342	90.250	46.445	69.630	32.954
0.00120	3.820	101.107	53.188	80.418	36.831
0.00135	4.297	114.119	59.933	94.148	43.615
0.00150	4.775	127.042	66.670	105.916	48.461
0.00165	5.252	140.073	73.504	120.627	54.277
0.00180	5.730	153.248	80.246	137.299	61.061
0.00195	6.207	166.501	87.107	151.029	-
0.00210	6.685	180.009	93.859	163.778	-
0.00225	7.162	193.439	100.788	184.373	-
0.00240	7.639	206.740	107.763	191.238	-
0.00255	8.116	-	-	207.910	-
0.00270	8.593	-	-	216.736	-

Table 3 – Table of results for pressure drop across the heat exchanger gained through simulation and experimentation

5.4. Error Analysis

Throughout the project it was important to consider any errors that could be encountered along the way.

Firstly, the temperature change experiment will have had errors associated with it. The digital screens on the HT30X heat exchanger service unit provided readings for hot and cold water volumetric flow rate, and the temperatures at all four inlets and outlets. Readings on these digital screens were provided to an accuracy of either 2 or 3 significant figures depending on the size of the measurement, which was equivalent to 2 decimal places for the flow rates and 1 decimal place for temperature. This means that the error of the volumetric flow rate

measurement was ±0.005 litres per minute, whilst for temperature the error was ±0.05°C – both evenly distributed, random errors. The value of volumetric flow rate also fluctuated slightly whilst measurements were being taken, creating an additional error of ±0.02 litres per minute. The errors mentioned for readings of volumetric flow rate were both absolute errors and thus to get the total error of each reading these two absolute errors must be summed, giving an error of ±0.025 litres per minute for each reading.

There were also errors that accompanied the modelling process. However, these errors were more to do with the simplification of the original CAD geometry and as such were difficult to quantify.

There were also some noteworthy errors in the pressure drop experiment, the first of which was related to parallax error. Measurements for head height were recorded by measuring from the centre of the meniscus at the top of the water, but the manometer board was located behind the HT30X heat exchanger service unit which made it difficult to ensure that all readings were taken with the centre of the meniscus directly at eye-level. This therefore introduced another random error, but quantification of parallax error can be tricky. It was estimated that the error presented by parallax was roughly ±2mm. The error for volumetric flow rate was the same as in the temperature drop experiment; ±0.025 litres per minute.

6. Discussion and conclusions

6.1. Discussion

The simulation results for pressure drop across each circuit of the heat exchanger provide a fairly close match to the results provided by the experimental work. However, the experimental values were all higher than the corresponding value from simulation, and this difference ranged between 10-20kPa for each value. The main reason for this is probably due to the simplifications made to the original CAD model provided by HiETA. The final CAD model had extremely simplified inlet and outlet manifolds, which will not have provided a hugely accurate representation of the real heat exchanger. However, for the purposes of this project the simplified model was sufficient considering the time limitations of the project and the processing power of the computers used for the simulations.

To add to this, the porous zone used for the simulations was not completely accurate. This was because, as discussed in the literature review, the porous zone of the heat exchanger consisted of hundreds of horizontal tubes – meaning that the resistance of the porous zone was different in each plane of reference, i.e. the zone was anisotropic. Due to time constrictions the porous zone was left as an isotropic region for every simulation and as a result of this these simulations will not have been as accurate as they potentially could have been.

Another point of note is that the hot and cold water circuits of the heat exchanger were analysed separately on ANSYS Fluent, rather than as one unit. The reason behind this was that, in order to correctly analyse the heat exchanger as one unit, the two separate sections needed to be linked using a complex temperature coupling equation so that the two sections were able to transfer heat between each other just like the heat exchanger would in reality. Unfortunately there was not enough time to investigate this, so this is another reason behind the differentiation between the modelling and experimental results for pressure drop.

Finally, analysis of the initial temperature change experiment showed that, for certain hot water flow rates in countercurrent flow, the mean temperature efficiency of the heat exchanger was greater than 100%. This is not possible, but there are a couple of factors that could explain why these efficiencies were calculated. Firstly, the heat exchanger – when arranged in countercurrent flow - was found to exchange heat extremely quickly, at a rate which was greater than the rate at which the HT30X service unit could reheat the water. This meant that the temperature readings for inlet and outlet temperature were constantly fluctuating and as such had to be read before they had properly settled. This may have led to some experimental errors which explains the lack of a smooth curve in Figure 14, which shows the temperature change across both circuits in countercurrent flow, and these experimental errors may be the reason that the calculated values for temperature efficiency were slightly peculiar.

Despite these abnormal results, it was still possible to obtain the optimum operating conditions out of all of the boundary conditions tested. Analysis of Tables 5 and 6 in Appendices A and B respectively revealed that an inlet flow rate of 0.445 m/s whilst the heat exchanger was arranged in countercurrent flow gave a mean temperature efficiency of 95%, whilst the pressure drop across the hot and cold water circuits were approximately 20kPa and 37kPa respectively. This was one of the highest achieved mean temperature efficiencies, whilst the pressure drop

was one of the lowest measured – meaning that the required fluid pumping power would also be relatively low; and this is a desirable property for an efficient heat exchanger.

6.2. Future Work

This project can be used in the future as a stepping stone for further investigation of the topics mentioned throughout this report.

Future work that could be of particular use would include the development of a temperature equation to link the hot and cold water circuits on ANSYS Fluent. This would mean that any simulations would provide results that are more realistic than those presented in this project and would hopefully be very similar to the experimental results gained within this report.

Another way to further improve the simulations by conducting further work would be to set up the porous zone as an anisotropic region in order to better replicate the conditions created by the tubes within the heat exchanger. This would require in depth research into how these tubes actually resist the flow of water so that accurate anisotropic conditions and a correct Darcy's law matrix could be created – as discussed in the literature review.

The pressure drop experiment could also be repeated with a more appropriate manometer so that results for all required flow rates could be measured for both the hot and cold water circuits.

7. Project management, consideration of sustainability and health and safety

The overall structure of the project was planned out at the end of term 1, using a Gantt chart to provide a visual representation of processes and time management. This Gantt chart can be seen in Figure 20 at the end of this section.

As is evident from the Gantt chart, weekly meetings with the project supervisor were scheduled – but in reality the dates of some meetings changed due to other commitments and practicalities. A logbook was taken to every meeting so that notes could be recorded for future reference, and it was also used to note any rough calculations, sketches or general information regarding the project. After each meeting, any new logbook material was copied into a word document so that a back-up of all the information was available in case the logbook were to be misplaced.

Also shown in the Gantt chart are the planned dates of both experiments. These experiments

were set to be completed by mid-February, and would hopefully be completed by Easter at the latest if any complications were to arise. However, due to unforeseen circumstances only the first experiment was completed before the Easter break and as a result of this the second experiment was completed at the start of term 3 – on the 25th April. In order to ensure that the project was still finished before the deadline, the whole project write-up that did not rely on the second experiment was written over the Easter break and any data from the second experiment was added on the 25th and 26th April – leaving one whole day for formatting and proofreading of the project before the submission date on the 28th April.

A risk assessment, which can be seen in Figure 19, was conducted prior to experimental work in order to identify any hazards associated with the experiment and how these risks could be mitigated.

Risk Assessment Form						
Name of person carrying out assessment	Andrew Farley					
Description	Experimental investigation into the temperature change and pressure drop across a compact heat exchanger at varying hot and cold water flow rates, with the aid of an HT30X heat exchanger service unit.					
Potential Hazard	**Who Could be Harmed?**	**How?**		**Likelihood**	**Severity**	**Risk Score**
High temperatures (surfaces + liquids)	Student	Burns to skin due to prolonged contact with hot surfaces or liquids.		3	2	6
Water borne hazards	Student	Contact with dirty water could lead to infection by harmful micro-organisms.		1	5	5
Electrical safety	Student	Failure of Residual Current Device (RSD) could lead to an electric shock.	Minor shock	2	1	2
			Large shock	1	5	5

Figure 19 - Risk assessment form; likelihood (1 - rare, 5 - almost certain); severity (1 - insignificant, 5 – catastrophic)

The service unit is capable of producing temperatures that could cause burns, and this was the highest scoring risk in the experimental risk assessment form – although scores of 6 out of a maximum 25 may still be treated as insignificant. In order to minimise this risk, it was ensured that the circulator unit was closed and secure while the equipment was in operation. The heater inside the circulator unit can remain at high temperatures for several minutes after operation has ended, and for this reason caution was exercised when opening and closing the circulator.

The second highest scoring risk was the danger presented by water borne diseases. Under certain conditions, scale, rust, algae or sludge can grow in the water and microscopic bacterium

such as Legionella pneumophila will feed on this and breed rapidly. If any water containing this bacterium is spilt airborne droplets can produce a form of pneumonia called Legionnaires Disease – and this is potentially fatal. In order to mitigate the risk of water borne diseases under the COSHH regulations, the water within the service unit must be changed regularly, the equipment must be cleaned regularly and – where practical – the water should be maintained at a temperature below 20°C.

The risk of electric shock was also considered, with the severity of shocks ranging from insignificant to potentially fatal – especially if combined with pre-existing medical conditions such as a weak heart. The service unit operates from a mains voltage electrical supply and contains a Residual Current Device (RCD). The purpose of the RCD is to cut the supply of electricity should the equipment become electrically dangerous through accident or misuse, and this will reduce the severity of any electric shock, and injury, that an operator may encounter. To minimise the risk of RCD failure, proper operation of the RCD must be checked at least monthly by pressing the 'TEST' button on the service unit. If the circuit breaker does not trip when the button is pressed, the equipment must be checked and repaired by a qualified electrician before it may be used.

In terms of the sustainability of the project, the heat exchanger was manufactured by HiETA using additive manufacturing techniques. Techniques such as this create very small amounts of waste, whilst the heat exchanger itself should last for several years so long as it is sensibly maintained and protected.

The entire purpose of designing a more efficient heat exchanger is to allow for the fabrication of more environmentally sustainable products, such as cars with lower fuel consumption and emissions. The long term environmental benefits gained by achieving greater efficiency of any heat exchange processes will hugely outweigh the energy required to design, manufacture and analyse cutting edge heat exchangers such as this one – and because of this, engineering operations such as this can certainly be classed as sustainable.

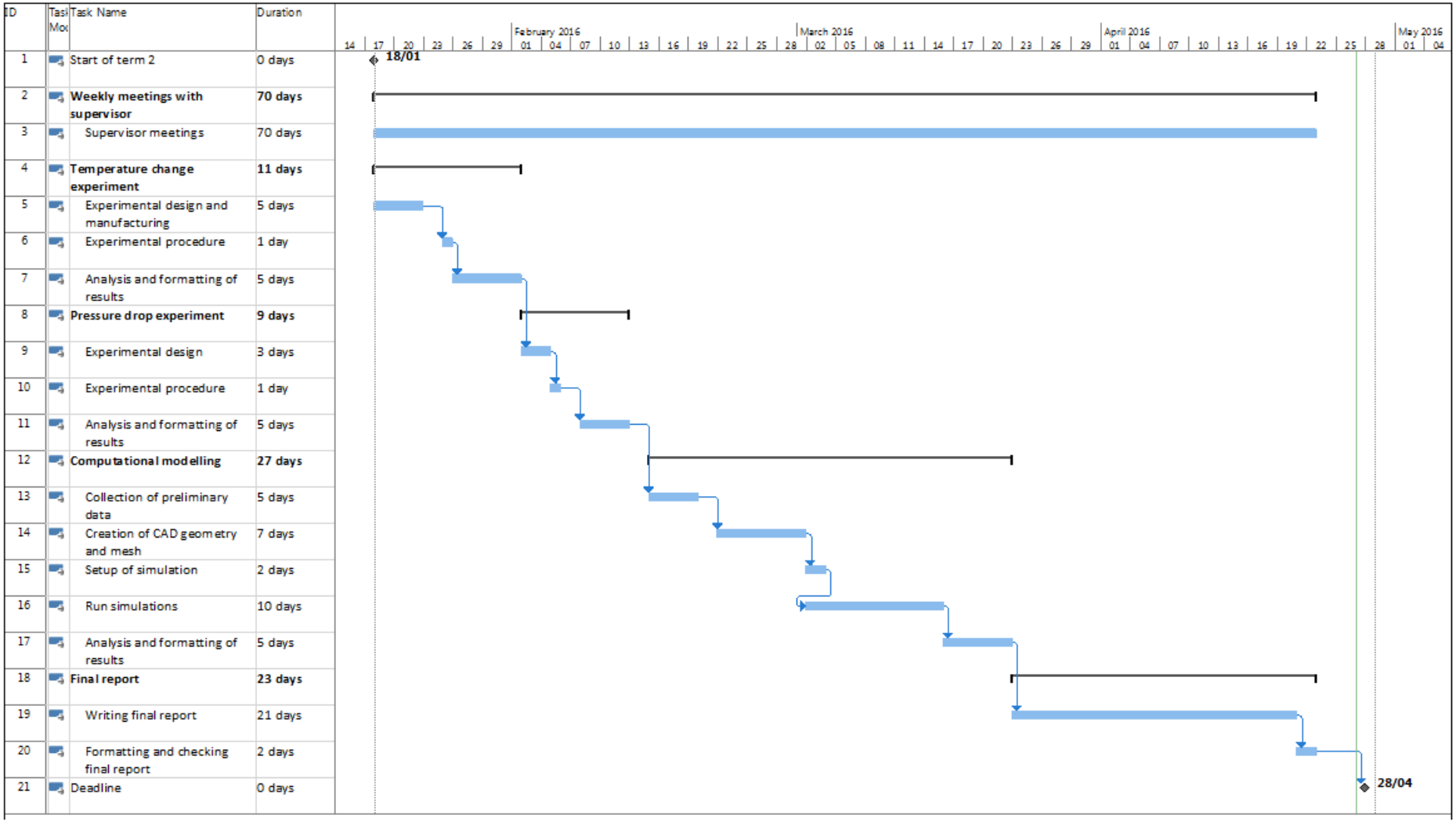

Figure 20 - Gantt chart

References

[1] Thermopedia. (2011) *Shell and Tube Heat Exchangers.* [Online] Available from: http://www.thermopedia.com/content/1121/

[2] Biotuning. (2013) *Parts Heat Exchangers.* [Online] Available from: *http://www.biotuning.co.uk/PartsHeatExchangers.htm*

[3] Process-Heating. (2016) *No more fouling the spiral heat exchanger*. [Online] Available from: *http://www.process-heating.com/articles/85208-no-more-fouling-the-spiral-heat-exchanger?v=preview*

[4] Slideshare. (2014) *Types of Heat Exchangers.* [Online] Available from: *http://www.slideshare.net/AjaykumarAsodariya/heat-exchanger-41154656*

[5] HiETA. (2016) *Case Studies and Collaboration Projects.* [Online] Available from: *http://www.hieta.biz/*

[6] Ramesh K Shah and Dusan P Sekulic (2003). *Fundamentals of Heat Exchanger Design*. New Jersey: John Wiley & Sons, Inc. 378-381.

[7] Mohammed M. Farid (2010). *Mathematical Modelling of Food Processing*. Florida: CRC Press. 205-209.

[8] W Sobieski (2010). *Examples of Using the Finite Volume Method for Modelling Fluid-Solid Systems*. Warsaw: University of Warmia and Mazury. 257-264.

[9] ANSYS Fluent User Guide. (2016) *Porous Media Modelling.* [Online] Available from: *http://www.afs.enea.it/project/neptunius/docs/fluent/html/ug/node233.htm*

[10] Thermopedia. (2011) *Darcy's Law.* [Online] Available from: *http://www.thermopedia.com/content/1047/*

[11] Compass. (2015) *Flow through porous media.* [Online] Available from: *http://www.compassis.com/downloads/Manuals/Porous_media.pdf*

[12] Checalc. (2016) *LMTD Calculator.* [Online] Available from: *http://checalc.com/solved/lmtd.html*

[13] Engineering Toolbox. (2015) *Heat Transfer Fluids.* [Online] Available from: *http://www.engineeringtoolbox.com/overall-heat-transfer-coefficient-d_434.html*

[14] Engineering Toolbox. (2015) *Properties of Water.* [Online] Available from: *http://www.engineeringtoolbox.com/water-density-specific-weight-d_595.html*

[15] Wikipedia. (2016) *Porosity.* [Online] Available from: *https://en.wikipedia.org/wiki/Porosity*